JOURNAL OF GUIDANCE, CONTROL, AND DYNAMICS
Vol. 17, No. 6, November–December 1994

Robust Control Design and Implementation on the Middeck Active Control Experiment

Simon Grocott,* Jonathan How,† David Miller,‡ Douglas MacMartin,§ and Ketao Liu¶
Massachusetts Institute of Technology, Cambridge, Massachusetts 02139

This paper presents a coherent methodology for robust controller synthesis for the Middeck Active Control Experiment (MACE): a Shuttle program scheduled for flight on STS-67 in February 1995. The experiment has been designed to investigate the extent to which the on-orbit behavior of a precision-controlled spacecraft can be predicted and controlled using analysis and ground testing prior to launch. A goal of the flight experiment is to demonstrate good payload pointing performance using active controllers designed based on the predicted structural dynamics. For systems with complicated control topologies and large model uncertainties, this requires a systematic control design methodology. The results from preliminary ground-based control experiments are used in this paper to present such a design technique and to illustrate how it can be applied to future flight experiments. This control design methodology is then used to develop controllers that obtain a 22 dB improvement in the performance metric on the current MACE hardware.

I. Introduction

As more stringent performance requirements are placed on future spacecraft, the resulting increase in control bandwidth requires that the structural flexibility of the system be considered, which is the Control-Structure Interaction (CSI) problem.[1] Structural flexibility presents a performance limitation on many current operational spacecraft,[2] but this can be overcome by controlling the modes of vibration. However, the accuracy to which the structural dynamics can be modeled limits the potential performance improvements. Very accurate models of the spacecraft dynamics can be directly measured during ground testing. However, these models typically include direct gravity and suspension effects that limit their usefulness for predicting the 0-g dynamics.[3–5] The on-orbit flexible behavior of a spacecraft can be predicted using analytic techniques [finite element models (FEMs)], but typically, these are not sufficiently accurate to be used for high-authority control.[6] On-orbit system identification of the spacecraft could also be performed, but it is then difficult to develop confidence in the final performance prior to launch.

The Middeck Active Control Experiment (MACE), scheduled for flight on STS-67 in February 1995, has been designed to address the modeling and control issues associated with the change in operational environment of a flexible spacecraft from 1-g to 0-g. To this end, the test article was designed to couple suspension and gravity effects with the flexible behavior during ground testing.[7] Because the system has 9 actuators, 17 sensors, and more than 50 modes within the control bandwidth, it is sufficiently complicated to require a new, programmatic approach to modeling and control design. Previous research and flight experiments indicate that this design approach should include analysis, ground tests, and on-orbit redesign.

The overall design process that has been developed for the MACE program is presented in the next section. This paper concentrates on the control design aspect of this process. The design of robust controllers is naturally iterative, so a design methodology is proposed that separates the synthesis process into its key steps. The first steps consist of identifying and investigating relevant subproblems of the overall design problem to provide a better understanding of the effects of the various design parameters. In the last steps, the compensators and the knowledge from the subproblems are combined to form controllers that address the overall performance objective.

The following sections provide a description of the MACE program. A preliminary set of control experiments are then discussed. The results from these tests are used to demonstrate the relevant design issues, illustrate some appropriate analysis tools, and motivate the design methodology. The approach is then formally presented and applied to a series of more complicated control experiments.

II. Middeck Active Control Experiment

1. MACE Science Objectives and Approach

The objective of MACE is to act as a pathfinder for a qualification procedure for flexible, precision-controlled spacecraft. This procedure will increase confidence in the eventual orbital performance of future spacecraft that cannot be dynamically tested on the ground in a sufficiently realistic zero-gravity simulation.[7]

The overall modeling and control procedure for MACE is illustrated in Fig. 1. Both finite element and measurement modeling techniques are used to exploit the advantages of each. A 1-g FEM is developed that includes gravity and suspension effects, and its accuracy is improved through modal identification and model updating (step A in Fig. 1). Because small errors in the open-loop dynamics can lead to large discrepancies between the experimental and predicted closed-loop behavior, further inaccuracies are identified by comparing the actual 1-g closed-loop performance with the model predictions (step B). Measurement models fitted to transfer function data tend to provide accurate estimates of the modal parameters of the test article and can be used to further update the physical parameters in the 1-g FEM (step C).[8] To complete the ground-based procedure, controllers are designed using the measurement models. By comparing the performance obtained with that achieved using finite-element-based controllers, the cost-benefit ratio of further FEM refinement can be determined (step D).

Next, by removing the gravity and suspension effects, the FEM can be used to predict the on-orbit system response (step E). Of course, even with the refinements to the 1-g FEM, there will still be a variety of errors in the 0-g model and thus the need for robust control.[5,6]

Control redesign using measurement models from an on-orbit system identification (step F) will then help to determine the limitations of predicting 0-g closed-loop behavior from analysis and ground testing and the performance benefits that can be realized

Received Dec. 7, 1993; revision received April 25, 1994; accepted for publication April 23, 1994.

*Graduate Student, Space Engineering Research Center. Student Member AIAA.
†Assistant Professor, Department of Aeronautics and Astronautics. Member AIAA.
‡Principal Research Scientist, Space Engineering Research Center. Member AIAA.
§Currently Research Engineer, United Technologies Research Center, East Hartford, CT. Member AIAA.
¶Postdoctoral Associate, Space Engineering Research Center. Member AIAA.

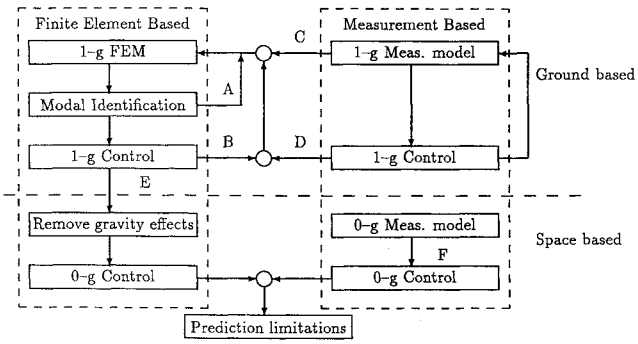

Fig. 1 Modeling and control for MACE.

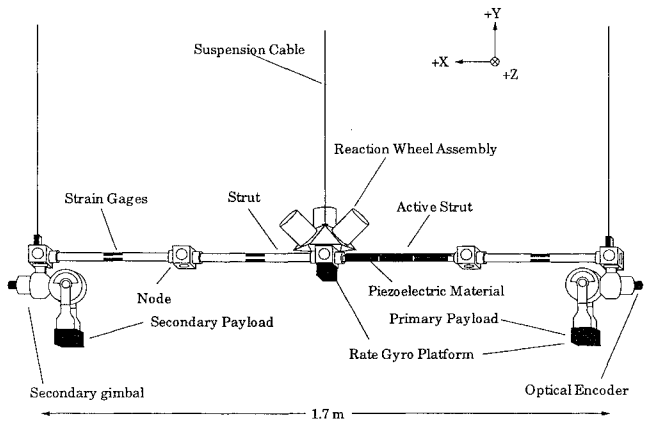

Fig. 2 MACE test article suspended in 1-*g* by a three-point suspension system.

through on-orbit identification and control redesign. Thus, the mission results from MACE will enable an assessment of the accuracy of 0-*g* FEM predictions as they pertain to precision control.

2. Hardware Description

The MACE test article was chosen to represent a precision-controlled, high-payload-mass fraction spacecraft, such as Earth-observing platforms, with multiple, independently pointing or scanning payloads.[2] The test article, shown schematically in Fig. 2, consists of a flexible bus to which two payloads, a reaction wheel assembly, and other actuators and sensors are mounted. Each payload is mounted to the structure using a two-axis gimbal that provides pointing capability. Instrumentation includes angle encoders on each gimbal axis, a three-axis rate gyro platform mounted under the reaction wheel assembly, and a two-axis rate gyro platform mounted in the primary payload. The bus is composed of circular cross-sectional Lexan struts connected by aluminum nodes. The structure is supported for ground tests by a pneumatic/electric low-frequency suspension system.[9]

Note that because the suspension cables, bus, and gravity vector all lie in the same plane, the dynamics of the structure naturally decouple into vertical (about the Z axis) and horizontal (about the XY axes) dynamics. This decoupling can be used to simplify the control design process.

The control is implemented using a real-time computer operating at a 500-Hz sampling rate. The combination of computational delay, zero-order hold, anti-aliasing filters, and sensor dynamics introduces a net time delay of 11 ms.

3. Measurement Model Formulation

All controllers discussed in this paper were designed using continuous-time measurement models of the test article in 1-*g*. Each model was derived by fitting measured transfer function data from the control actuators (u) and disturbance sources (w) to all of the feedback sensors (y) and performance variables (z) using an algorithm that minimizes the mean-square difference in the logarithm of the modeled and measured transfer functions.[10] The transfer functions were measured through the real-time computer to include processing delay. The transfer function matrix $G(s)$ for the system is partitioned as

$$G(s) = \begin{bmatrix} G_{zw}(s) & G_{zu}(s) \\ G_{yw}(s) & G_{yu}(s) \end{bmatrix} \tag{1}$$

Although measurement models are very accurate, several sources of error still exist. First, the data include noise, so the fits are never exact. Second, deviations between the model and the system occur at frequencies below 0.5 Hz, where measurement data are sparse, and at high frequencies due to unmodeled modes. Also, the test article exhibits nonlinearities due to small fluctuations in the suspension system and friction in the gimbal motors. Furthermore, the frequencies of the test article change after disassembly and reassembly. These modeling errors are smaller than the errors between the FEM and the actual structural dynamics but still have a substantial impact on the control design and the performance that can be achieved.

The structural dynamics of MACE, combined with sensor dynamics, result in a fast roll-off of the transfer functions in most control channels. As a result, high-frequency unmodeled dynamics are not as important as parameter uncertainties, such as variations in the frequencies of the lightly damped poles and zeros. It is difficult to directly treat uncertainty in zero frequencies. However, experience indicates that because altering the frequencies of poles has a significant effect on the system zeros, it is sufficient to limit the model of uncertainty to the eigenvalues of the system.

As discussed earlier, the purpose of this paper is to focus on the control design methodology. To enable a detailed discussion of the performance-robustness issues, the relatively accurate measurement models will be used for controller design. The design methodology is applied to the more complicated case of finite-element-based controllers in Ref. 6.

III. Control Design and Analysis Techniques

The control objective is to design a reduced-order control law $u = G_c y$ that minimizes the $\mathcal{H}_2$ (quadratic) norm of the closed-loop transfer function matrix from disturbance to performance. The overall MACE performance criterion is to minimize the root-mean-square (rms) payload inertial angles, as estimated by integrating the rate gyro measurements, in response to white-noise disturbances applied to the secondary gimbal.

Although optimal in the sense of performance on the model, the actual performance of linear quadratic Gaussian (LQG)[11] controllers on MACE is limited by the lack of robustness to parameter uncertainties. Reducing control authority does introduce robustness, but it does so in an ad hoc and conservative manner. Robust techniques will, by their very nature, reduce the performance that can be achieved on the design model. However, because the resulting controllers are less sensitive to model errors, they should obtain better performance on the test article.

Several robust control design techniques, including sensitivity-weighted LQG (SWLQG),[12] maximum entropy (ME),[13] multiple model (MM),[14] and Popov controller synthesis,[15] have been investigated. These control synthesis algorithms are listed in increasing order of guaranteed robustness and also in increasing order of computational effort. Note that there are typically many degrees of freedom in the robust control synthesis problem. These include the relative sensor noise intensities and actuator penalties that are often used to trade off performance for robustness. Furthermore, with the robust control techniques, the parameters to be treated as uncertain must be selected and sized. Thus, to avoid wasted effort, a coherent methodology is required to design controllers that achieve good robust performance on a complicated system such as MACE.

Note that because the MACE performance problem is characterized by an rms ($\mathcal{H}_2$) performance objective and real parameter uncertainty, the problem does not easily fit into either the $\mathcal{H}_\infty$ or μ robust control frameworks.[16]

With any control technique, the design must be analyzed to check performance and stability robustness on the design and evaluation models and, if available, open-loop data collected from the test arti-

cle. Because the data are more representative of the system than the models, it can be used to obtain good predictions of the expected performance. The data can also be used to identify robustness problems, which speeds up the design process because not all of the designed controllers have to be implemented on the hardware.

Performance graphs are very useful for evaluating frequency regions with stability or performance robustness problems. Controllers are compared by plotting the state cost

$$J_{xx} = \int_{-\infty}^{+\infty} \mathrm{tr}[G_l^*(j\omega) R_{xx} G_{\mathrm{cl}}(j\omega)]\, \mathrm{d}\omega \qquad (2)$$

where the weighting matrix R_{xx} contains the relative contributions of the performance variables, and $G_{\mathrm{cl}}(s)$ is a frequency-domain representation of the closed-loop system. The square root of the integrand of this cost is then plotted vs frequency. A comparison of open- and closed-loop performance using the design model and the data reveals frequency regimes where model errors impact performance.

The multivariable Nichols test is an effective means of predicting stability of the closed-loop system. With a stable plant and compensator, stability of the closed-loop system is checked by determining if the plot of

$$H_n(j\omega) = -1 + \det[I + G_{yu}(j\omega) G_c(j\omega)] \qquad (3)$$

where G_{yu} is the system response from the actuators to the sensors, lies to the right and below the critical points $-1 \pm 2m\pi$, $m = 0, 1, \ldots, \infty$. This plot is particularly useful if the curves based on the model and the open-loop data are compared directly. The multivariable Nichols test directly indicates stability but not robustness. However, a plot of

$$H_s(j\omega) = \sigma_{\min}[I + G_{yu}(j\omega) G_c(j\omega)] \qquad (4)$$

can be used to obtain a measure of the sensitivity of the closed-loop system. The singular-value plot can also be used to identify problems such as compensator-zeros/plant-poles with mismatched frequencies. Large discrepancies between the singular values as computed on the model and on the data can indicate a potentially destabilizing model error that requires a more robust compensator.

All of these control design and analysis techniques play an integral role in the control design methodology presented in Sec. V. The extension of these procedures to include analysis techniques for systems with real parameter uncertainty is discussed in Refs. 6, 12, 15.

IV. Preliminary Experiments

Preliminary experiments were instrumental in refining the modeling, design, and evaluation tools. They also provided an indication of the robustness issues (mismodeling, nonrepeatability, and nonlinearities) that have to be addressed when the controllers are based on measurement models. The experience acquired through these experiments led to the development of the design methodology for robust multivariable controllers presented herein.

The impact of model errors on the control design depend on two key features of the control problem. One is the control topology. Here, we adopt the notation in Ref. 17 and classify the topology as standard (nondegenerate), input degenerate, output degenerate, or input-output degenerate, depending on the location and type of the various sensors and actuators. For example, an input-degenerate system has disturbance sources and actuators that influence the same degrees of freedom, thus giving the control direct authority over the disturbance. Similarly, an output-degenerate system has sensors that directly measure the performance variables. Although degenerate topologies are preferable, many real problems are nondegenerate, and these are the most interesting and difficult control problems.

A second issue is the dimensionality of the G_{yu} feedback loop, i.e., the number of sensors and actuators. The key difficulty is determining the correct relative weighting between the sensors and actuators. An incorrect choice of weights could lead to a controller that overemphasizes a particular control loop. If this loop is based on model dynamics that are particularly uncertain, the controller could be very sensitive to model errors. However, by balancing the controller effort with respect to the uncertainty, one might be able to obtain similar performance with a more robust compensator.

Table 1 Sensor and actuator suite for preliminary control problems

Test	w	u	y	z
SISO gimbal	PGz	PGz	PRGzi	PRGzi
SIMO gimbal	PGz	PGz	BRGzi	PRGzi
			PENz	BRGzi
MIMO reaction wheel	RWx	RWx	BRGxi	BRGxi
	RWy	RWy	BRGyi	BRGyi
	RWz	RWz	BRGzi	BRGzi
MIMO gimbal and reaction wheel	SGz	PGz	PENz	PRGzi
		RWz	BRGzi	BRGzi

Abbreviations: SISO, single input, single output; MIMO, multi-input, multi-output; PG, primary gimbal motor; SG, secondary gimbal motor; RW, reaction wheel; PRG, payload rate gyro; BRG, bus rate gyro; PEN, primary gimbal encoder; x, y, z, bus axis of orientation; i, band-limited integration.

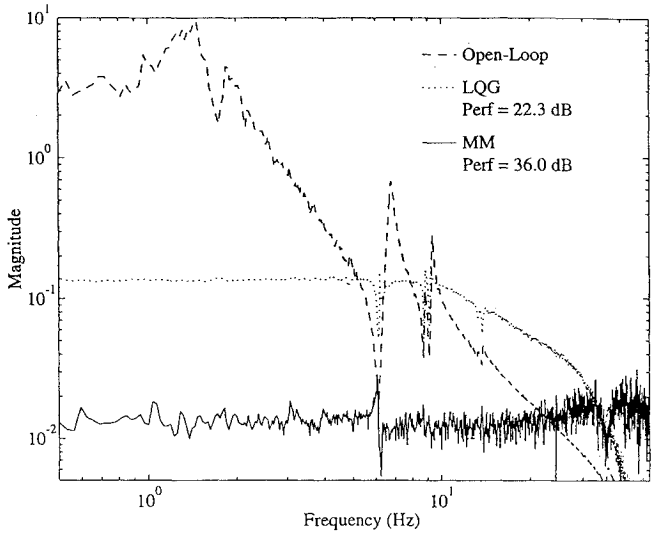

Fig. 3 Performance frequency response for SISO gimbal control problem.

1. Single-Input, Single-Output Gimbal Control

The overall MACE control objective is to minimize the rms inertial angle of the primary payload when disturbed by a broadband, small-angle excitation of the secondary gimbal. Because the primary gimbal exerts the most authority over the inertial angle of the payload, a single-axis control loop using this actuator was explored first.

The sensor and actuator suite for this and all the preliminary experiments is given in Table 1. Only motion about the Z axis was excited and controlled by the input-output degenerate sensor and actuator in this experiment. The open-loop G_{zw} transfer function, shown in Fig. 3, is dominated by the payload pendulum and first bending modes at 1.4 and 1.7 Hz, respectively, which simplifies the control design.

To improve the rms pointing performance, several LQG controllers with increasing control authority were implemented. At moderate levels of control authority, errors in the model of a suspension cable violin mode at 9 Hz limited the LQG compensator to a 22 dB performance improvement. The robustness was improved using the multiple-model technique with a stable compensator constraint. Two models were used for the design. One with the 9 Hz mode shifted slightly lower, and the second with the mode slightly higher in frequency. The results in Fig. 3 show the 36 dB reduction in inertial payload pointing error experimentally achieved using this robust controller.

Notice that the SISO, dominant-mode, input-output degenerate system had only a minor robustness concern due to uncertainty/nonrepeatability in the frequency of the suspension violin mode at 9 Hz. When the sensitivity of the controller to this uncertainty was reduced, the performance was dramatically increased until limited only by lags in the system and sensor noise. Thus, sys-

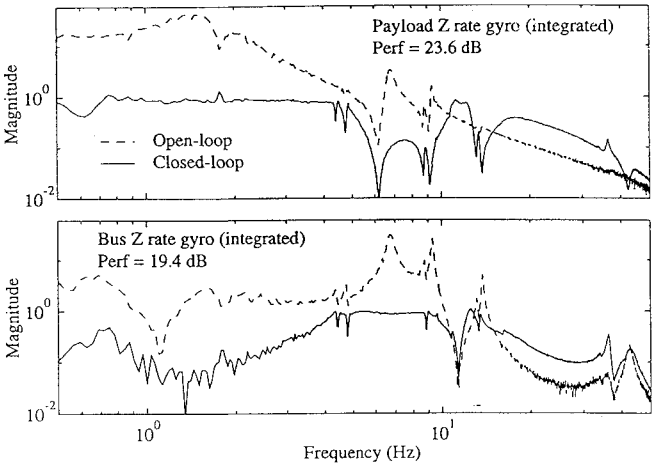

Fig. 4 Performance frequency response for the SIMO gimbal control problem.

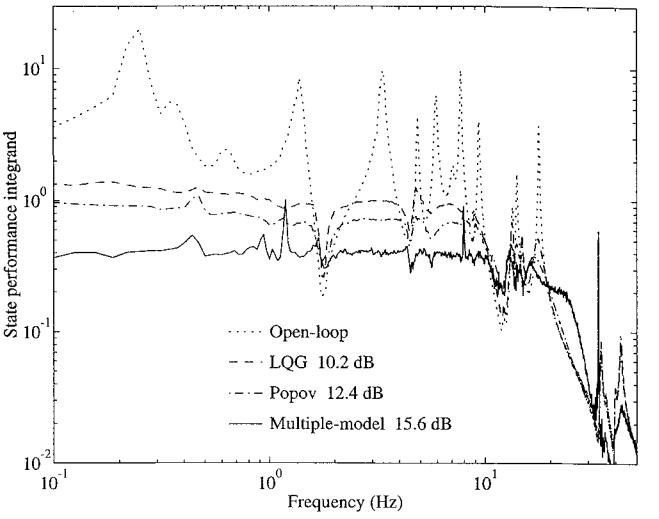

Fig. 5 Integrand of state cost function in Eq. (2) for the MIMO reaction wheel control problem. Performance comparison of several MIMO robust controllers.

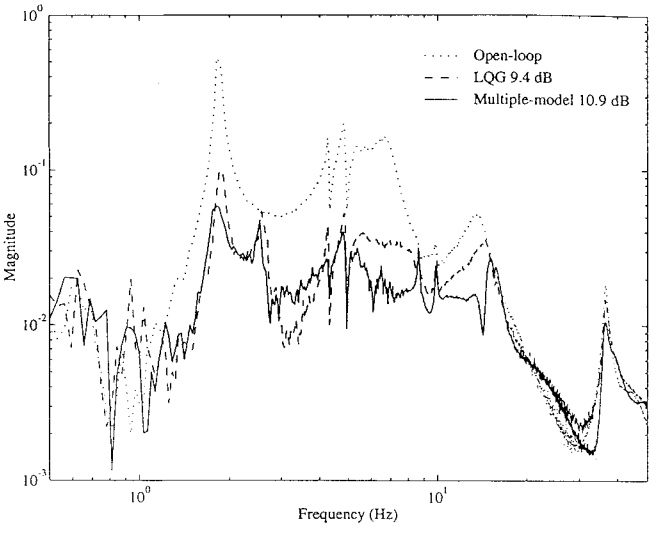

Fig. 6 MACE Z-axis performance using LQG and multiple-model approaches on MIMO gimbal and reaction wheel control problem.

tems that exhibit these three features are relatively easy to robustly control at high levels of authority.

2. Single-Input, Multiple-Output Gimbal Control

The second experiment considered a system with the same disturbance source, actuators, and performance metric, but with different sensors. This SIMO system is input-degenerate, so the controller must infer the performance variable from the two measured sensors and the structural dynamics. Initial tests showed that reducing the bus sensor noise resulted in control designs that strongly depended on the structural model and, as a result, were very sensitive to modeling errors. Several combinations of weights were compared, but the model errors near 9 Hz limited the LQG performance improvement to 20 dB, which is similar to that achieved with a direct-feedback measurement of the performance.

During these first two control experiments, it was observed that the bus motion increased as the gimbal reacted against the structure to isolate the payload. To reduce this effect, both the payload and bus motion were penalized in the control objective. For this new performance metric, the open-loop frequency responses of G_{zw} are shown in Fig. 4. Due to the relative symmetry of the test article, the first bending mode at 1.7 Hz is almost unobservable to the Z-axis bus rate gyro. The payload pendulum mode is also barely observable due to its localized behavior.

The closed-loop results in Fig. 4 show that LQG controllers suppressed the payload pointing error and bus vibration by more than 20 dB. Thus, although performance is not dominated by one or two modes, this input-degenerate SIMO system resulted in few robustness problems because the gimbal can cancel the disturbance at the source.

3. MIMO Reaction Wheel Control

The next experiment investigated control using the reaction wheels. This MIMO system is input-output degenerate but does not exhibit the dominant-mode characteristic of the previous two examples. Figure 5 compares the open-loop state response and the closed-loop performance achieved using LQG, MM, and Popov compensators. As indicated, the best experimental closed-loop performance with an LQG controller was 10.2 dB. Without resorting to either a stability constraint or unstable compensation, a Popov controller was designed that yielded a 12.4-dB reduction in the rms bus motion. With a stability constraint on the compensator, a MM controller achieved a 15.6-dB performance improvement but resulted in some lightly damped compensator poles. These modes increased the sensitivity to modeling error and resulted in sharp peaks in the performance autospectra at 1 and 8 Hz. A model error at 33 Hz was also encountered that limited further performance improvements.

These results demonstrated that the non-dominant-mode nature of the problem complicated the control design at high frequencies and reduced the performance improvements that could be achieved.

4. Gimbal and Reaction Wheel Control

The final preliminary experiment investigated a nondegenerate system with no dominant modes. In this test, all four gimbal motors have proportional-integral servos (bandwidth of 3 Hz). These servos use the encoder signals for feedback and were designed to represent a conventional payload pointing control system. At low frequency, the actuator input commands relative gimbal angle.

Figure 6 compares the open-loop and the best closed-loop performance obtained using LQG and MM compensators that obtained 9.4 and 10.9 dB performance improvements, respectively. Significant differences between predicted and actual performance occurred below 6 Hz, especially for the LQG controller. Also, the first bending mode is almost unobservable/uncontrollable in the feedback loop. As a result, the controller must estimate the system response at this frequency using the system model, making the designs very susceptible to model errors.

A further complication results due to nondegeneracy. Simply increasing the overall gain of the controller does not necessarily result in improved performance. Instead, a delicate balance between actuator inputs and structural dynamics must be achieved, and this was found to have serious robustness implications.

Thus, in conclusion, input-output, degenerate SISO systems that have dominant modes were found to be the most tolerant to model errors. Systems with many modes that contribute to the performance

and feedback loops tend to require higher bandwidth controllers, which typically results in significant robustness problems as the compensator rolls off in the presence of time delay. The nondegenerate problem places a high reliance on the model to accurately describe the coupling between the disturbances, actuators, sensors, and performance variables. Finally, MIMO topologies can result in noncollocated feedback channels whose robustness strongly depends on design model accuracy.

This sequence of experiments was presented to illustrate the important role that preliminary tests play in understanding robust control design. These experiments identified dynamics that were uncertain, techniques for reducing their impact on closed-loop performance, and observability/controllability issues. In addition, this exercise revealed a design process that allows the efficient selection of the numerous design parameters that comprise the overall MACE problem.

V. Control Design Methodology

In this section, we distinguish between the design process and the specific algorithms such as modeling codes, control formulations, and analysis techniques. The purpose of this control design process is to determine good sensor/actuator topologies, the relative weights in the performance objective, and appropriate uncertainty models.

It is possible to determine a priori some of the control design parameters, such as error models and relative sensor noises. However, a complete investigation of the design parameters requires an iterative approach using the analysis tools discussed previously. Of course, to expedite the design process, these iterations must be performed on simpler and smaller systems than the overall MACE problem.

The resulting design approach consists of five main steps:

1) Formulate the overall performance problem.
2) Identify important subproblems for this system.
3) Thoroughly investigate each subproblem.
4) Combine the results from step 3.
5) Solve and evaluate the overall performance problem.

Note that steps 2 and 3 and steps 4 and 5 tend to be iterative. Furthermore, after completing and evaluating the result in step 5, it may be necessary to iterate back to any previous step including possibly reformulating the performance objective.

In the framework of MIMO control, formulating the original problem means that a model of the plant exists, the sensors and actuators have been chosen, and the disturbances and performance metric have been identified. The principle of step 2 is that a better understanding of the effects of each parameter can be obtained by studying several subsets of the parameters rather than the whole set. These lower order problems permit faster iterations, and a better understanding of the parameters reduces the number of iterations required for the overall system. For example, a collocated sensor and actuator pair can be studied to determine the relationship between control weights and sensor noise intensities and their effect on robustness and performance levels. As illustrated in the previous sections, considerable simplifications in the system dynamics can be achieved by selecting the sensors and actuators to form an output-degenerate system with dominant-mode behavior. Also, on systems such as MACE, low-order problems arise due to geometric decoupling between the axes (XY-axes and Z-axis).

Once determined, each subproblem must be investigated thoroughly. There are three objectives at this stage. The first is to determine values for the control parameters that result in "good" controllers that exhibit low sensitivities on the model and the data. For simplicity, this initial step is usually done using LQG. The control penalty and sensor noise intensity are then varied to develop an understanding of their effects on each control loop. The second objective is to identify the plant uncertainties that most affect the closed-loop stability and performance and determine how these problems can be fixed using a simple robust control technique, such as SWLQG. The emphasis here is on simple techniques, so that many iterations can be performed quickly. More advanced techniques can be used when solving the final performance problem. Using SWLQG, the control authority is gradually increased so that further robustness problems can be identified. The main objective of this process is to investigate the performance limitations associated with each subproblem and determine how these difficulties will be reflected in the overall objective.

The results of each of these subproblems can then be combined in several ways to formulate compensators for more complex control topologies. In the next section, knowledge from the subproblems is used to combine the controllers by slowly increasing the authority of the additional control loops associated with the added sensors and actuators. A second approach is just to physically combine the state-space representations of the controllers and then perform a balanced reduction. In either case, several iterations are usually required to completely investigate the interactions between the controllers developed for the subproblems. This typically includes analyzing the effect of changing relative control penalties and the robustness of adding extra sensors and actuators. Ultimately, the purpose of step 4 is to develop a sufficient understanding of the MIMO control problem to allow an efficient design of a compensator for the overall performance objective, which corresponds to step 5. The final designs must also be evaluated to determine the effects of the controller on other aspects of the spacecraft motion. For example, one of the compensators in the preliminary experiments achieved good performance using payload isolation, but at the expense of increasing the bus vibration. This problem was solved by reformulating the performance objective to include an additional penalty on the bus motion.

One should note that this design approach is not intended to replace detailed modeling with extensive iteration on control design. It is just a more flexible approach to control design that increases the designer's understanding of the critical issues, reduces the complexity of design parameter selection, and reduces the total time required to design controllers.

VI. Experimental Illustration of Design Process

This design process will be illustrated by extending previous control results to the XY axes of the MACE test article. In this case, in addition to the four gimbal servos, a relative speed control reaction wheel servo (bandwidth of approximately 2 Hz) was included to improve linearity. The performance values in this example are with respect to the servoed system. Of course, the servos also contribute to the actual performance objective. To avoid potential difficulties with saturation and system nonlinearities, the compensators in this study were restricted to be stable.[17]

1. Formulate

The sensors and actuators for this overall XY-axes problem are given in Table 2. The four-input, three-output measurement model contains 62 states. The main purpose of this study was to determine the most efficient use of the sensors and actuators in order to obtain a robust compensator that yields good rms performance on the test article. Note that this performance objective penalizes only the payload inertial angle.

2. Identify

Three main SISO subproblems were identified, based on the collocated sensor-actuator pairs. For each subproblem, the disturbance w and the performance z are the same as in the overall problem. Thus, the results of each subproblem provide a clear indication of the capabilities of each sensor and actuator pair for the overall performance problem in Table 2.

Table 2 Sensor and actuator suite for overall problem (XY-axes) (notation defined in Table 1)

Test	w	u	y	z
Overall XY-axes	SGx	PGx	PRGx	PRGxi
		RWx	BRGx	
		RWy	BRGy	
Subproblem 1	SGx	PGx	PRGxi	PRGxi
Subproblem 2	SGx	RWx	BRGx	PRGxi
Subproblem 3	SGx	RWy	BRGy	PRGxi

3. Investigate

The first subproblem is quite similar to the SISO gimbal preliminary experiment. However, because the disturbance input and actuator are not collocated but the performance and sensor are, the problem is output degenerate and some of the dominant-mode behavior is lost. With the experience from the preliminary tests, there were few robustness/performance difficulties with this configuration. By adjusting the control weights and sensor noise intensities, an LQG controller was designed that yielded a 12.2 dB performance improvement in the rms payload motion. Unstable controllers resulted at higher authority.

The second subproblem was much more difficult because the system is nondegenerate. However, the reduced observability/controllability discussed in the last preliminary test on the Z axis was not a factor in the XY-axes dynamics. The initial design for this subproblem also used feedback of the stabilized integral of the rate gyro measurement. However, only 5 dB performance improvement could be achieved using a stable LQG compensator. Higher authority designs placed unstable compensator poles near the frequency of the stabilized integrators (0.03 Hz). This problem was avoided by removing the integrator and feeding back the rate gyro signal directly. With this modification, a performance improvement of 10 dB was achieved before LQG compensator stability again became an issue.

An ad hoc approach to stabilizing the compensator is to treat the structural modes near the frequency of the unstable pole as uncertain. Using this approach with the SWLQG, a stable compensator was designed that achieved a 12.3 dB performance improvement. The closed-loop results indicated that this sensor/actuator pair could not control all of the modes in the bandwidth of interest. Thus, further designs were halted pending the results of the third subproblem.

Analysis of the third subproblem indicated that the Y-axis sensor/actuator pair alone was not particularly effective for the overall performance objective, but it can be used to control the modes at 7.5 and 20 Hz. This result was found to be most important once significant authority had been exerted on the dominant modes by the X-axis actuators.

4. Combine

The results from these three subproblems were then used to develop a controller for the overall problem. The combination process started with the best X-axis reaction wheel design. The authority of the Y-axis control loop was then gradually increased by reducing the weights on the appropriate sensor and actuator, yielding a good understanding of the interaction between the two control loops. For the final reaction wheel XY-axes controller, Fig. 7 compares the predicted closed-loop results based on the design model and the open-loop data. In general, the agreement is very good, but there are some discrepancies in the 3–10 Hz range. These predictions are also compared with the experimental results, which show a 15.2 dB performance improvement. As expected, the predictions based on the open-loop data agree very well with the experimental results, clearly illustrating the power of this analysis tool as part of the design process. The performance improvement over the original X-axis controller was achieved primarily by exerting authority on the modes at 7.5 and 20 Hz using the Y-axis reaction wheel and bus rate gyro as seen in the third subproblem.

In the second combination step, the payload rate gyro and primary gimbal were introduced to this reaction wheel XY-axes controller by gradually reducing the sensor noise and control weight. Note that in this case, in contrast to the first subproblem, the rate gyro was fed back directly, so some additional iteration was required at this stage. The controllers resulting from this combination step finally addressed the overall XY-axes problem and represent the beginning of the final step in the design methodology.

5. Solve

Some further refinements to these designs were required to address some performance and robustness problems. Figure 8 shows the multivariable Nichols test for one of the initial controllers for the overall problem. The test was performed using both the measurement model and the measured open-loop data. Both tests indicate that the closed-loop system will be stable. However, this controller

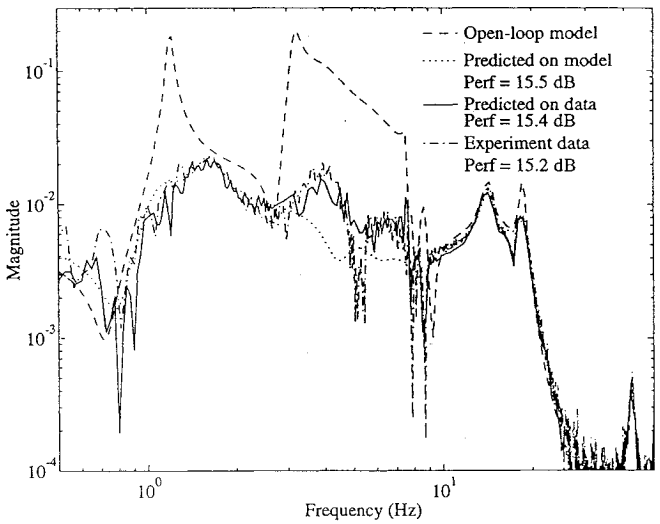

Fig. 7 Frequency response from X-axis secondary gimbal to X-axis primary payload rate gyro (integrated) using the XY-axes reaction wheel controller. Closed-loop experimental data compared to performance predicted by model and on open-loop data.

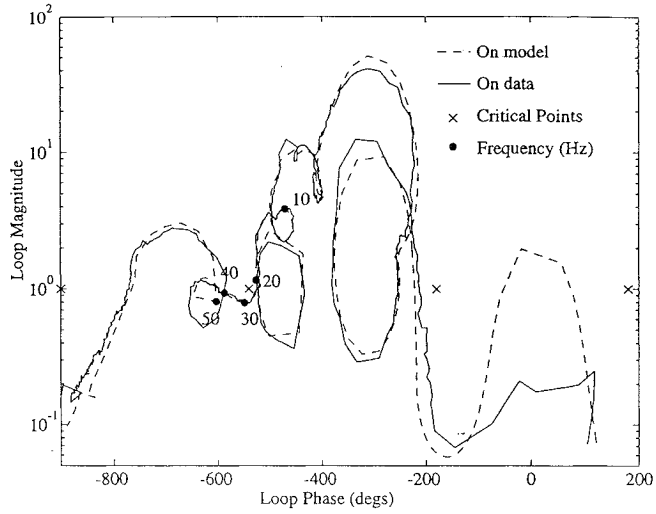

Fig. 8 Nichols plot for XY-axes controller.

was implemented on the test article and a stability problem was experienced at approximately 50 Hz. Figure 8 indicates that the plot of $H_n(s)$ is close to the critical point (-1) in the 20–30 Hz region, but not in the 40–50 Hz range. Thus, the Nichols plot does not predict any implementation difficulties in that frequency range.

A second analysis technique based on the singular values of $I+G_{yu}G_c$ is shown in Fig. 9. The graph compares the three singular values as predicted on the model and on the open-loop data. The minimum singular values (bottom curve) also indicate some sensitivity in the 20 Hz range, as might be expected from the proximity of the loop response to the critical point in Fig. 8. Note that the model and data both agree on the magnitude of the singular values in this frequency range. However, the discrepancy between the model and the data at approximately 50 Hz is striking. The singular values as computed using the data appear to indicate that there is a mismatch in the frequency of a plant pole and a compensator zero. An additional sensitivity weight on the mode at 50 Hz was included to account for this problem, and the redesigned controller achieved good performance. At this performance level, bus motion was relatively more pronounced. Thus, the overall problem in Table 2 was reformulated to include the bus inertial angles as performance variables, as in the preliminary SIMO gimbal control problem.

A further extension of these results was to design a significantly reduced-order controller using the multiple-model robust control technique. The previous SWLQG controllers were truncated to approximately 48 states for implementation on the hardware. To

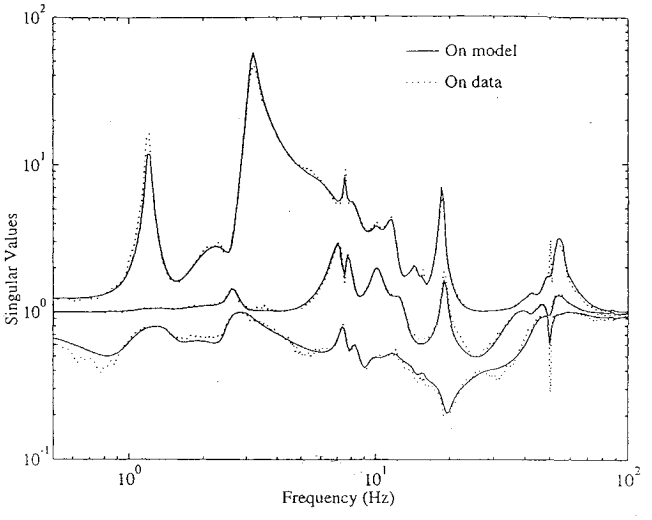

Fig. 9 Singular values of $I + G_{yu}G_c$ for XY-axes controller.

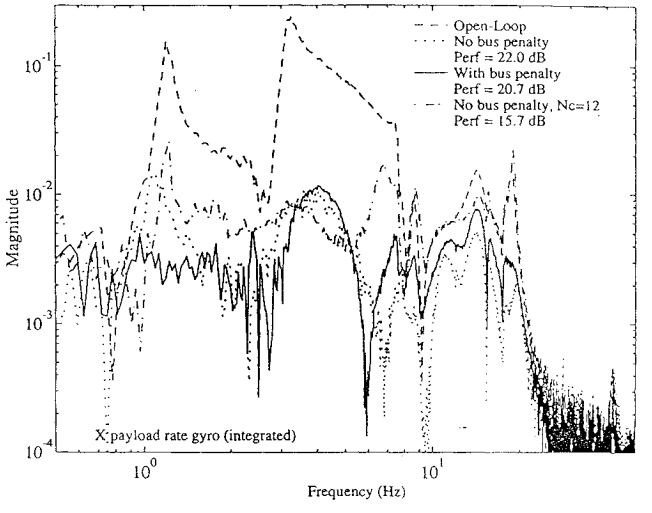

Fig. 10 Frequency response from X-axis secondary gimbal to X-axis primary payload rate gyro (integrated) using several XY-axes controllers (reaction wheel and gimbal).

investigate the potential limitations of low-order compensators, an optimal MIMO controller with only 12 states ($N_c = 12$) was also developed for this system.

The closed-loop results for the overall problem with these XY-axes controllers are shown in Fig. 10. The compensator designed with only a penalty on the payload inertial angle achieved a performance improvement of 22.0 dB, whereas the compensator designed with a penalty on the bus and payload angles achieved an improvement of 20.7 dB in the payload inertial angle. However, this second compensator reduced the bus motion by 9.5 dB, compared to the 3.7 dB of the first design. Note that there are key differences in the closed-loop frequency responses in the 1–3 Hz and 10–20 Hz ranges. The reduced-order compensator achieved a performance improvement of 15.7 dB. A comparison with the higher order designs shows that the closed-loop response is similar below 5 Hz but much worse in the 5–20 Hz range. The payload pointing performance improvements achieved during the design process are summarized in Table 3.

This control example clearly illustrates the design methodology of Sec. V. The results show that designing simple SISO loops with the correct performance metric is an excellent way to gain knowledge of the fundamental abilities and limitations of each sensor-actuator pair. Combining these SISO loops to form more complicated MIMO loops can then be done incrementally until the MIMO problem is fully understood. When possible, it is most constructive to start with the simplest control algorithms (LQG) and to switch to more complicated algorithms as robustness issues necessitate. This design

Table 3 Experimental performance improvement (secondary gimbal disturbance to payload inertial angle) at different stages of the design process

Problem	Improvement, dB
Subproblem 1	12.2
Subproblem 2	12.3
Subproblem 3	2.0
2 and 3 combination	15.2
Overall XY axis	
No bus penalty	22.0
With bus penalty	20.7
Reduced order	15.7

methodology is used in Ref. 6 to design XYZ-axes controllers using the MACE FEM, which has significant real parameter uncertainty.

VII. Conclusions

The Middeck Active Control Experiment is an excellent testbed for investigating the design of active controllers for future spacecraft. The flight experiment analyzes various modeling and control issues for both ground and space-based operations. This paper focuses on an effective control design methodology for large-order systems with many sensors and actuators. The design process uses several control formulations, evaluation tools, and a coherent sequence of subproblems to efficiently formulate robust multivariable controllers. The approach was used on MACE to design controllers that obtain an order of magnitude improvement in payload inertial pointing performance.

Acknowledgments

The authors thank Payload Systems Inc. and Lockheed Missiles and Space Company. The program is supported by the NASA Langley Research Center and the NASA In-Step Office, with Gregory Stover as technical monitor.

References

[1]Junkins, J. L., *Mechanics and Control of Space Structures*, AIAA, Washington, DC, 1990.

[2]McLaren, M. D., and Chu, P. Y., "Slew Disturbance Compensation for Multiple Payloads of a Flexible Spacecraft," *Proceedings of the AIAA Guidance, Navigation, and Control Conference*, AIAA, Washington, DC, pp. 668–679.

[3]Crawley, E. F., Barlow, M. S., van Schoor, M. C., and Bicos, A. S., "Variation in the Modal Parameters of Space Structures," in *Proceedings of the 33rd AIAA/ASME/ASCE/AHS Structures, Structural Dynamics, and Materials Conference* (Dallas, TX), AIAA, Washington, DC, 1992, pp. 1212–1228.

[4]Bukley, A. P., Patterson, A. F., Anderson, J. B., and Driskill, T. C., "Reduced Gravity Multibody Dynamics Testing," in *AAS Guidance Navigation and Control Conference*, edited by R. Culp and R. Rausch, Vol. 86, Keystone, Colorado, pp. 331–342, Feb. 1994.

[5]Glaese, R., and Miller, D. W., "On-Orbit Modeling of the Middeck Active Control Experiment from 1-g Analysis and Experimentation," paper presented at the *12th International Modal Analysis Conference (IMAC)*, pp. 1107–1113, Feb. 1994.

[6]How, J. P., Glaese, R. M., Grocott, S. C. O., and Miller, D. W., "Finite Element Model Based Robust Controllers for the MIT Middeck Active Control Experiment (MACE)," *Proceedings of the American Control Conference*, Inst. of Electrical and Electronics Engineers, Piscataway, NJ, 1994, pp. 272–277.

[7]Miller, D. W., Sepe, R. B., Saarmaa, E., and Crawley, E. F., "The Middeck Active Control Experiment (MACE)," paper presented at the 5th NASA/DOD CSI Technical Conference, Tahoe, CA, March 1992, pp. 551–565.

[8]Glaese, R. M., "Development of Zero-Gravity Structural Models from Analysis and Ground Experimentation," Thesis, Dept. of Aeronautics and Astronautics, Massachusetts Inst. of Technology, Cambridge, MA, Jan. 1994 (MIT SERC Report #3-94).

[9]Kienholtz, D. A., "A Pneumatic/Electric Suspension System for Simulating On-Orbit Conditions," American Society of Mechanical Engineers, ASME 90-WA/AERO-8, Dallas, TX, Nov. 1990.

[10]Jacques, R. N., and Miller, D. W., "Multivariable Model Identification from Frequency Response Data," *Proceedings of the IEEE Conference on Decision and Control* (San Antonio, TX), Inst. of Electrical and Electronics Engineers, Piscataway, NJ, 1993, pp. 3046–3051.

[11]Kwakernaak, H., and Sivan, R., *Linear Optimal Control Systems*, Wiley-Interscience, New York, 1972.

[12]Grocott, S. C. O., "Comparison of Control Techniques for Robust Performance on Uncertain Structural Systems," M.S. Thesis, Department of Aeronautics and Astronautics, Massachusetts Inst. of Technology, Cambridge, MA, Jan. 1994 (MIT SERC Report 2-94).

[13]Hyland, D. C., "Maximum Entropy Stochastic Approach to Controller Design for Uncertain Structural Systems," *Proceedings of the American Control Conference* (Arlington, VA), June 1982, pp. 680–688.

[14]Ashkenazi, A., and Bryson, A. E., Jr., "Control Logic for Parameter Insensitivity and Disturbance Attenuation," *Journal of Guidance, Control, and Dynamics*, Vol. 5, 1982, pp. 383–388.

[15]How, J. P., Hall, S. R., and Haddad, W. M., "Robust Controllers for the Middeck Active Control Experiment Using Popov Controller Synthesis," *IEEE Transactions on Control Systems Technology*, Vol. 2, June 1994, pp. 73–87.

[16]Doyle, J. C., "Analysis of Feedback Systems with Structured Uncertainties," *IEE Proceedings*, Vol. 129, Part D, 1982, pp. 242–250.

[17]MacMartin, D. G., and How, J. P., "Implementation and Prevention of Optimal Unstable Compensators," in *Proceedings of the American Control Conference*, Inst. of Electrical and Electronics Engineers, Piscataway, NJ, June 1994, pp. 1290–1295.